CHEMICAL ENGINEERING TRANSACTIONS
VOL. 114, 2024
A publication of AIDIC
The Italian Association of Chemical Engineering
Online at www.cetjournal.it
Guest Editors: Petar S. Varbanov, Min Zeng, Yee Van Fan, Xuechao Wang

ISBN 979-12-81206-12-0; **ISSN** 2283-9216
DOI: 10.3303/CET24114013

Synthesis of N-best Heat Recovery Networks with Consideration of Dynamic Control Performance

Zong Yang Kong[a], Tiffany Ang[b], Hao-Yeh Lee[c,d]*, Ákos Orosz[e], Ferenc Friedler[f], Bing Shen How[b,]*

[a]School of Engineering and Technology, Sunway University, Petaling Jaya 47500, Malaysia
[b]Research Centre for Sustainable Technologies, Swinburne University of Technology, Kuching, Malaysia
[c]National Taiwan University of Science and Technology, Department of Chemical Engineering, Taipei City, Taiwan
[d]National Taiwan University of Science and Technology, Process Net-Zero Center, 43 Keelung Rd., Taipei City,Taiwan
[e]Department of Computer Science and Systems Technology, University of Pannonia, Veszprém, Hungary
[f]Széchenyi István University, Egyetem tér 1, 9026 Győr, Hungary
haoyehlee@mail.ntust.edu.tw; bshow@swinburne.edu.my

Recently, graph-theoretic methods have increasingly been employed to generate near-best (n-best) heat recovery networks, aiming to maximize energy recovery efficiency. The exploration of these n-best networks has proven pivotal for making informed decisions. Nevertheless, existing studies in this domain have not attempted to study the favourability of these generated networks based on their respective dynamic control performance. This performance metric reflects the network's ability to maintain target temperature even under disturbances. The network topologies play important role in both economic (i.e., total annual cost (TAC)) and dynamic control aspects. To address this gap, this work introduces a hybrid approach. First, all combinatorically feasible heat recovery networks are generated using P-HENS. Thereafter, each network undergoes dynamic control performance evaluation through Aspen Plus simulations. The final step involves optimization of the network structures based on fuzzy method which avoids over-prioritization. To illustrate the efficacy of the proposed methodology, it is applied to solve a 5-stream problem. Results showed that Network A with the least TAC ($122,249) is not necessarily associated with the greatest dynamic performance (with failure rate of 15 %). Network C which offers the balance performance (with TAC of $122,666 and failure rate of 0 %) is chosen.

1. Introduction

Based on a recently published Global Carbon Budget report, carbon emissions attributed to fossil fuels hit a high peak in 2023, i.e., about 1.1 % greater than that in year 2022 (Abnett, 2023). This calls for pragmatic solutions to enhance the overall energy efficiency by maximizing the energy recovery. Process Integration (PI) tools are widely applied to reduce the overall energy consumption which further contributes to emissions reduction. This is achieved by forming a heat recovery network (HRN) that exchanges thermal energy between the hot and cold streams among various processes.

Since the first systematic guide for HRN had been publicized by Linhoff and Flower (1985), its development has continuously progressed. The methodologies have progressively extended to address a broader scale of problems, including but not limited to multi-period operation (Oliveira et al., 2023), network retrofitting (Zahra et al., 2023), flexible network (Hafizan et al., 2019), and dynamic performance (Ghaderi et al., 2023). Nevertheless, most of the methodologies are designed to determine a single optimal solution which may not essentially be the most practical solution (Tan et al., 2024). Given the fact that the determined near-best (n-best) solutions can offer vital insights for decision-makers in making informed decisions (Voll et al., 2015), more attention has been placed towards exploring multi-solution heat exchanger network synthesis. For example, COMBINET method is used to discover multiple near-optimal networks (Mikkelsen and Qvale, 2001). Pavão et al. (2017), on the other hand, introduced a hybrid meta-heuristic approach that incorporates the use of Simulated Annealing and Particle Swarm Optimization to generate a list of feasible HRN for large-scale problems.

Paper Received: 15 June 2024; Revised: 28 October 2024; Accepted: 14 November 2024
Please cite this article as: Kong Z.Y., Ang T., Lee H.-Y., Orosz Á., Friedler F., How B.S., 2024, Synthesis of N-best Heat Recovery Networks with Consideration of Dynamic Control Performance, Chemical Engineering Transactions, 114, 73-78 DOI:10.3303/CET24114013

Recently, graph-theoretic based approach (i.e., P-HENS) has gained more interest as it can generate all combinatorically feasible networks that can meet the maximum energy recovery (MER) (Orosz and Friedler, 2020). Its effectiveness has been demonstrated through a series of successful engineering (Teng et al., 2023) and pedagogical (How et al., 2023) applications. A recent comparative study (Burgos et al., 2023) has confirmed the strength of P-HENS in yielding n-best networks that meet the MER goal, as compared to other market-available tools. Despite the positive outcomes, most works merely focus on elucidating its capability in generating all n-best networks but the systematic approach to further distinguish the generated networks is seldom discussed. Since the ability to ensure functionality of the network under disturbance is an important factor to ensure the system robustness (Kerlin and Upadhyaya, 2019), it is imperative to ensure the selected network is dynamically feasible. To achieve this, a hybrid approach that incorporates P-HENS and Aspen Plus Dynamics has been proposed to synthesize networks which are both economically and dynamically feasible.

2. Problem Statement

Given a set of hot stream *i* and a set of cold stream *j* where each hot stream is associated with a given heat capacity of CP_i and supply temperature of T_i^{Supply}; while each cold stream is associated with a given heat capacity of CP_j and supply temperature of T_j^{Supply}. Heat is exchanged through a series of process heat exchangers (connecting the hot and cold stream) and utility heat exchanger (i.e., heater and cooler) to meet the target temperature for both hot streams (T_i^{Target}) and cold streams (T_j^{Target}). A list of feasible HRNs *k*, which meet the minimum hot and cold utility ($Q^{hot,min}$ and $Q^{cold,min}$) are then determined. The work aims to determine the optimal HRN with the consideration of the total annual cost (TAC) and the dynamic performance (i.e., the ability to withstand a given disturbance in both supply temperature and flowrate).

3. Methodology

A three-step sequential procedure (Figure 1) is developed to solve the proposed problem. The general descriptions of each step are stated in the sub-sections below:

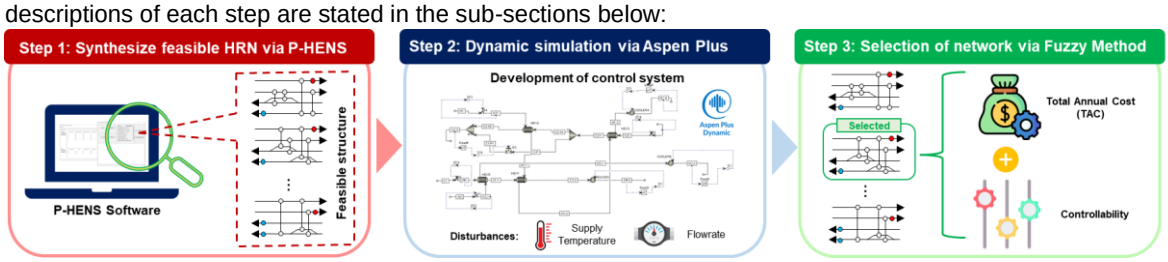

Figure 1: Proposed research methodology.

3.1 Step 1: Synthesis of n-best heat recovery network (HRN) using P-HENS

P-HENS is an extension of P-graph which are designed to generate combinatorically feasible solutions for HRN synthesis problems. Generally, the limiting data including stream (e.g., heat capacity, supply temperature, and target temperature for all involved hot stream *i* and cold stream *j*) and utility information (e.g., unit cost and supply temperature) are used as the input for the P-HENS software, where the feasible networks that able to meet the (i) temperature constraint (i.e., meeting the target temperature for both hot and cold stream while ensuring the minimum temperature difference between the two matching streams (ΔT^{min}) are maintained at a desired level) and (ii) pinch minimal energy constraint. At this stage, the identified network is ranked merely based on TAC which encompasses the utility costs and capital expenses. Eq(1) shows the TAC calculation of each determined network *k* (TAC_k), where C^{hot} and C^{cold} refer to the unit cost of hot and cold utility; while C^{HE} is the function of capital cost of heat exchangers which is a function of heat transfer area (A).

$$TAC_k = \left[Q^{hot,min} \times C^{hot} + Q^{cold,min} \times C^{cold} + \sum C^{HE}(A)\right]_k \quad (1)$$

3.2 Step 2: Dynamic performance evaluation using Aspen Plus Dynamics

In this step, the ability of each selected network to handle disturbances is tested by simulating the network using Aspen Plus Dynamics. Generally, the process begins with simulating the established network in Aspen Plus. Within this environment, HeatX is used to model the heat exchanger unit while the Heater component models both the heater and cooler units in the HRN. For all HeatX units, the hot stream outlet temperature is chosen as

the design specification. Once the HRN is established in Aspen Plus, it is then converted into a dynamic simulation *via* flow-driven simulation. The dynamic performance evaluation was done by introducing positive and negative disturbances in terms of temperature (±5 °C) and flowrate (±10 %) on all streams involved. In this work, the dynamic performance is expressed using two indicators: (i) failure rate which reflects the robustness of the network (FR_k) in tackling each disturbance scenario (lower failure rate means greater robustness) and (ii) worst-case temperature deviation (ΔT^{worst}) which indicates the greatest offsets of target temperature:

$$FR_k = \frac{N_k^{Fail}}{N^{Total}} \tag{2}$$

$$\Delta T^{worst} = \max\left(\left|T_i^{Target} - T_i^{Dis\_Target}\right|, \left|T_j^{Target} - T_j^{Dis\_Target}\right|\right) \tag{3}$$

where N_k^{Fail} refers to the number of failures where the target temperature is unable to achieved by a given control system; N^{Total} refers to the total number of disturbance scenarios; while $T_i^{Dis\_Target}$ and $T_j^{Dis\_Target}$ indicate the target temperature achieved for hot stream *i* and cold stream *j* when encountering disturbances.

3.3 Step 3: Multi-objective optimization

Finally, Fuzzy Optimization (FO) is opted as the strategy to rank the yielded HRNs with consideration of both TAC and dynamic performance. As the objective function of FO is to maximize the least satisfied objective (λ), it has a tendency to avoid over-prioritisation due to human bias (Tan et al., 2021).

$$max\ \lambda \leq [\lambda_a]_k \tag{4}$$

$$[\lambda_a]_k = \frac{P_a^{max} - [P_a]_k}{P_a^{max} - P_a^{min}} \tag{5}$$

where λ_a refers to the degree of satisfaction of performance indicator *a*, which can be computed using the max-min normalization method shown in Eq(5); $[P_a]_k$ refers to the performance scale of indicator *a* for network *k*; while the corresponding upper and lower limits are denoted as P_a^{max} and P_a^{min}.

4. Case Study

A 5-stream problem from Smith (2005) is modified and adopted as the case study in this work. The respective limiting data is shown in Table 1, while the other assumed parameters are summarized in Table 2.

Table 1: Limiting data of the proposed case study

Stream ID	Supply Temperature (°C)	Target Temperature (°C)	Heat Capacity (MW/°C)
H1	160	40	0.030
H2	150	50	0.050
H3	140	110	0.050
C1	60	160	0.050
C2	60	150	0.020

Table 2: Other parameters used in P-HENS

Item	Value	Reference	Item	Value	Reference
C^{hot} (\$/kWy)	37.64	P-HENS default value	$C^{HE}(A)$ (\$/y)	$145.63 \times A^{0.6}$	P-HENS default value
C^{cold} (\$/kWy)	18.12	P-HENS default value	ΔT^{min} (°C)	10	-

The generated network is then modelled in Aspen Plus Dynamics for dynamic performance evaluation. It is important to note that this work, by no means, aims to determine the optimal control strategy for each network but rather serves as an essential guide to incorporate dynamic control performance in n-best HRNs evaluation. With that, the same control strategy (inspired by Luyben et al. (1999)) is applied to the synthesized n-best HRNs. Specifically, bypass is installed across the heat exchanger to enable degree-of-freedom for process control, especially when it is connected with stream that does not contain any utility heat exchanger. The bypass fraction is set arbitrarily at 0.1 for all simulated networks to ensure the comparison of networks are made under identical conditions.

5. Results and Discussions

Figure 2 shows the 3 n-best HRN generated from P-HENS. Despite associating with different network topologies, all the networks can meet the pinch minimal energy constraint (i.e., 4.2 MW of $Q^{cold,min}$ and 0.9 MW of $Q^{hot,min}$). The corresponding TACs for both networks are tabulated in Table 3.

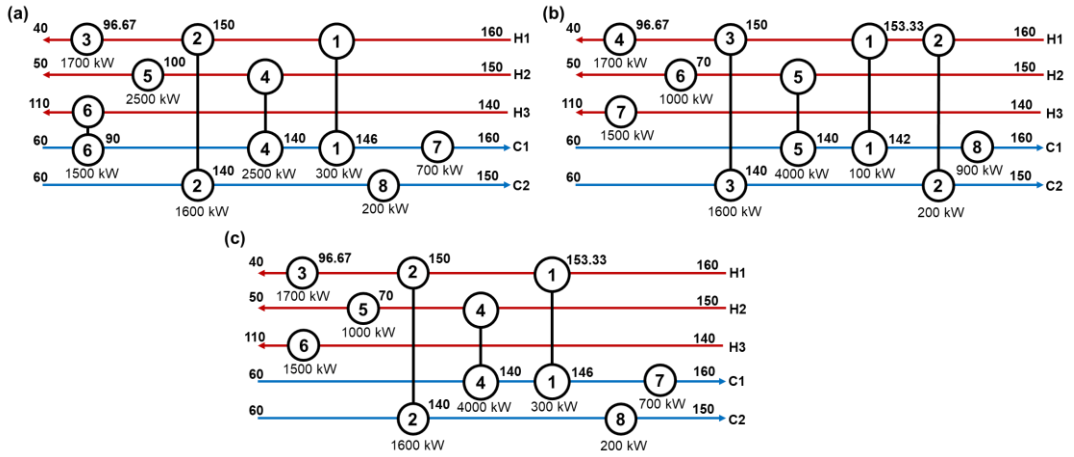

Figure 2: HRN generated from P-HENS: (a) Network A, (b) Network B, and (c) Network C (Numerical values represents temperature (°C) unless specified otherwise).

Table 3: Performance of each network generated from P-HENS and base case.

Network ID	TAC_k ($/y)	FR_k (%)	ΔT^{worst} (°C)	λ
A	122,249	15	2.96	0.338
B	122,913	35	4.47	0.000
C	122,666	0	0	0.372

Figure 3 illustrates the established control structures for all three networks, while Table 4 provides a summary of the dynamic performance evaluation. For Network A, it can restore the outlet temperature to its nominal value for 17 disturbance scenarios (out of 20), resulting in an FR_k of 15 %. Note that Network A fails to restore the outlet temperature when subjected to a +10 % feed flowrate on stream H3 and a +5 °C temperature increase on both stream H3 and C1. This outcome is expected because streams H3 and C1 feed into the same heat exchanger, whose outlet serves as the main control variable. As this outlet does not have a utility heat exchanger, any disturbance introduced upstream can significantly impact the outlet temperature, thereby influencing the dynamic performance of Network A. Among the 3 disturbances that prevent the outlet temperature from returning to its nominal value, the +5 °C on H3 exhibits the most significant ΔT^{worst} (i.e., 2.96 °C). For Network B, the FR_k is relatively high at 35 %, as the control structure can only restore the outlet temperature to its nominal value for 13 disturbance scenarios. There are 3 other disturbances that can bring the outlet temperature close to its nominal value (within 1°C), while the remaining 4 lead to a complete failure to restore the outlet temperature. Similar to Network A, disturbances that cause the outlet temperature to deviate from its nominal value are associated with the same heat exchanger, where the outlet serves as the main control variable. These disturbances include a −10 % feed flowrate on stream H1, a +10 % feed flowrate on stream C2, and a ±5 °C temperature change on H1. As previously discussed, the absence of a utility heat exchanger at this outlet appears to be the main factors that causes significantly impact of any upstream disturbance on the outlet temperature. Among the four disturbances that prevent the outlet temperature from returning to its nominal value, the +5 °C increase on H1 results in the most significant ΔT^{worst} of 4.47 °C. Regarding Network C, the FR_k stands out as the most favorable at 0 %. Consequently, all outlet temperatures can revert to their respective nominal values irrespective of the type of disturbances introduced. Consequently, in this network, there is no ΔT^{worst}, highlighting its robust performance in maintaining outlet temperature under varying conditions. This outcome is somehow expected due to all 5 streams in Network C feature a hot/cold utility heat exchanger at the outlet stream, which facilitate the restoration of outlet temperatures back to its nominal values, albeit to different amount of heating/cooling utility consumption.

In summary, the comparison of dynamic performance between all 3 networks indicates that Network C exhibits superior performance, as evidenced by the lowest FR_k and ΔT^{worst}. This was attributed to the presence of the hot/cold utility heat exchanger in all the 5 streams as explained previously. Following closely is Network A, with

a FR_k of 15 % and a ΔT^{worst} of 2.96 °C. One possible explanation for this could be attributed to its slightly less complex structure in comparison to Network B. From Figure 3(a), it is apparent that H3 serves as the main control variable, given the absence of process utility on that stream. In H3, there is only one heat exchanger along the stream. Consequently, the inlet of H3 passes through only heat exchanger #6, and the outlet temperature from this heat exchanger #6 serves as the main control variable. Although disturbances introduced to H3 may impact the output temperature, they are less likely to significantly affect other streams. Conversely, in Network B, the main control variable is situated on stream C2, which has two heat exchangers (#2 and #3) along the stream. Notably, these heat exchangers are closely linked to heat exchanger #1, leading to a more complex control structure and a potential "chain-effect" relationship between C2 and H1. Any disturbance in H1 could adversely affect C2, as H1 first exchanges heat with C2 *via* heat exchanger #2 and then undergoes another heat exchange with C2 *via* heat exchanger #3. This complexity complicates the entire network and likely contributes to the relatively poorer dynamic performance observed, characterized by the high FR_k . Consequently, achieving better and more robust control for Network B may be necessary to improve dynamic performance.

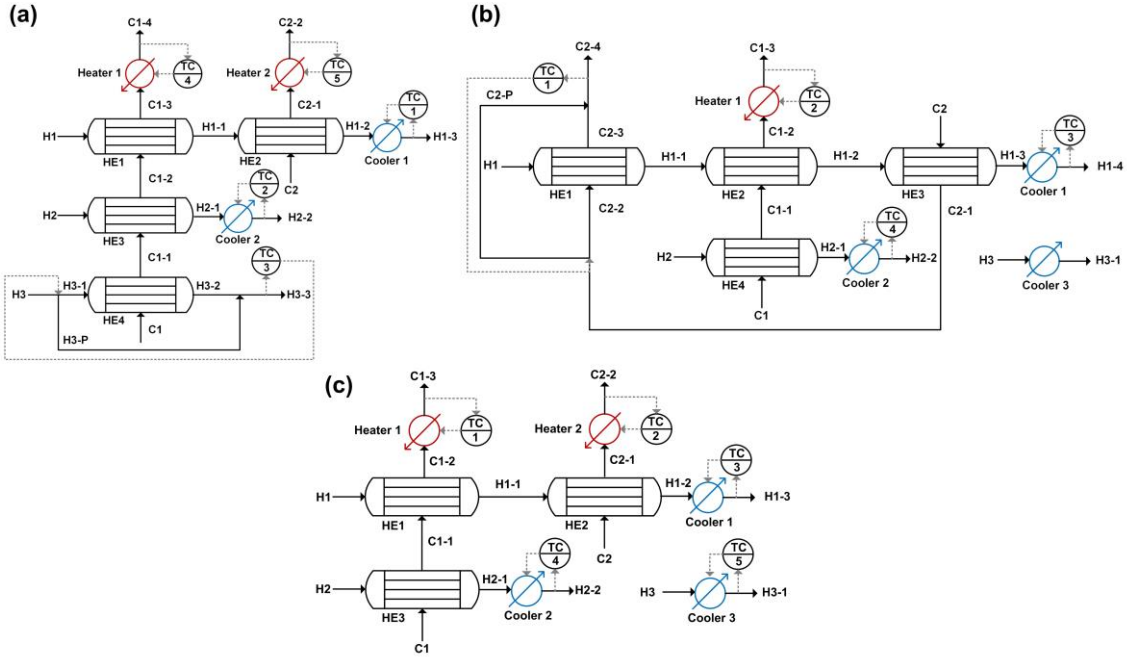

Figure 3: Control structures for (a) Network A, (b) Network B, and (c) Network C.

Based on FO, Network C with the highest λ is deemed as the optimal solutions. Despite its lower TAC as compared to Network A, the greatest satisfaction of Network C in both FR_k and ΔT^{worst}, causing it to become the most compromised solution. The case study has revealed that a network with the lowest TAC is not necessarily associated with the best dynamic control performances. In other words, this justifies the rationale of incorporating the proposed FO in the future applications.

6. Conclusions

Overall, this study presents a comprehensive framework for evaluating HRNs, emphasizing both cost-efficiency and operational robustness. Utilizing a 5-stream problem as a case study, 3 n-best HRNs were generated through P-HENS and subsequently simulated in Aspen Plus Dynamics for dynamic performance evaluation. Each network underwent testing with identical control strategies and disturbances, including temperature (±5 °C) and flowrate fluctuations (±10 %) across all streams. The dynamic performance indicators include the FR_k and ΔT^{worst}, under various disturbance scenarios, while FO was employed to rank HRNs based on both TAC and dynamic performance. Network C demonstrated the best dynamic performance, restoring all the outlet temperature back to its nominal value under all 20 disturbance scenarios. This is followed by Network A, which demonstrate the capability to restore the outlet temperatures to nominal values in 17 out of 20 disturbance scenarios, with a FR_k of 15 % and a ΔT^{worst} of 2.96 °C. Conversely, Network B exhibited the highest FR_k of 35 %, achieving nominal outlet temperatures in only 13 scenarios, with a ΔT^{worst} of 4.47 °C. It can be seen when the outlet temperature of Networks A and B fails to revert to its nominal value, it typically occurs under scenarios

where disturbances are introduced into a specific stream whose outlet functions as the primary control variable. Due to the absence of a utility heat exchanger at the outlet, disturbances introduced upstream can markedly affect the outlet temperature, consequently impacting the dynamic performance of both networks. According to FO, Network C with the highest λ is deemed as the optimal solution. Despite its lower TAC compared to Network A, the greater satisfaction of Network C in both FR_k and ΔT^{worst} causes it to become the most compromised solution. The current methodology measures the network's capability to address one disturbance at a time and its applicability is restricted to single-period operation problems. Future extensions can focus on extending the framework to cover (i) dynamic performance under multi-disturbance consideration and (ii) multiperiod control.

Acknowledgments

Authors would like to acknowledge financial support by Swinburne University of Technology Sarawak Campus via Research Seed Grant.

References

Abnett K., 2023, Global CO_2 emissions from fossil fuels to hit record high in 2023 -report, Reuters <www.reuters.com/business/environment/global-co2-emissions-fossil-fuels-hit-record-high-2023-report-2023-12-05> accessed 21.01.2024.

Burgos D., Valencia S., Amaya-Gómez R., Ratkovich N., 2023, Critique – Comparison between P-HENS and Aspen Energy Analyzer for heat exchanger network synthesis, Education for Chemical Engineers, 43, 113-114.

Ghaderi M., Reddick C., Sorin M., 2023, A Systematic Heat Recovery Approach for Designing Integrated Heating, Cooling, and Ventilation Systems for Greenhouses, Energies, 16(14), 5493.

Hafizan A.M., Alwi S.R.W., Manan Z.A., Klemeš J.J., Hamid M.K.A., 2019, Cost Optimisation of a Flexible Heat Exchanger Network with Fluctuation Probability using Break-Even Analysis, Chemical Engineering Transactions, 76, 403-408.

How B.S., Teng S.Y., Orosz Á., Sunarso J., Friedler F., 2023, Enabling in-depth analysis in heat exchanger network synthesis via graph-theoretic tool: Experiences in Swinburne University of Technology Sarawak Campus, Education for Chemical Engineers, 43, 100-112.

Kerlin T.W., Upadhyaya B.R., 2019, Dynamics and Control of Nuclear Reactors, Academic Press, Elsevier Inc., London, U.K.

Linnhoff B., Flower J.R., 1985, Synthesis of heat exchanger networks: I. Systematic generation of energy optimal network, AIChE Journal, 13, 107-119.

Mikkelsen J., Qvale B., 2001, A Combinatorial Method for the Automatic Generation of Multiple, Near-Optimal Heat Exchanger Networks, Chemical Engineering Research and Design, 79(6), 663-672.

Oliveira C.M., Cruz A.J.G., Costa C.B.B., 2023, Improving the Integrated Process of First- and Second-Generation Ethanol Production with Multiperiod Energy Integration, BioEnergy Research, 16, 1990-2011.

Orosz Á., Friedler F., 2020, Multiple-solution heat exchanger network synthesis for enabling the best industrial implementation, Energy, 208, 118330.

Pavão L.V., Costa C.B.B., Ravagnani M.A.S.S., 2017, Heat Exchanger Network Synthesis without stream splits using parallelized and simplified simulated Annealing and Particle Swarm Optimization, Chemical Engineering Science, 158, 96-107.

Smith R., 2005, Chemical Process Design and Integration, John Wiley & Sons Ltd., West Sussex, England.

Tan A.S.T., Uthayakumar H., Yeo L.S., Kong G.H., Lo S.L.Y., Andiappan V., Loy A.C.M., Teng S.Y., How B.S., 2024, Shapley-Shubik Agents Within Superstructure-Based Recycling Model: Circular Economy Approaches for Fish Waste Eco-Industrial Park, Process Integration and Optimization for Sustainability, DOI: https://link.springer.com/article/10.1007/s41660-024-00391-w.

Tan Y.D., Lim J.S., Andiappan V., Alwi S.R.W., Tan R.R., 2021, Shapley-Shubik Index incorporated debottlenecking framework for sustainable food-energy-water nexus optimised palm oil-based complex, Journal of Cleaner Production, 309, 127437.

Teng S.Y., Orosz Á., How, Jansen J.J., Friedler F., 2023, Retrofit heat exchanger network optimization via graph-theoretical approach: Pinch-bounded N-best solutions allows positional swapping, Energy 283, 129029.

Voll P., Jennings M., Hennen M., Shah N., Bardow A., 2015, The optimum is not enough: A near-optimal solution paradigm for energy systems synthesis, Energy, 82, 446-456.

Luyben W.L., Luyben, Tyréus B.D., Luyben M.L., 1999, Plantwide Process Control, McGraw-Hill, U.S.

Zahra P., Hadi S., Mehrab F.S., Reza H., Behnaz M.M., 2023, A novel relatively linear hybrid Three-Level strategy for retrofitting heat exchanger networks, Chemical Engineering Science, 265, 118213.